Determining the Intermolecular Structure in the S$_0$ and S$_1$ States of the Phenol Dimer by Rotationally Resolved Electronic Spectroscopy

Michael Schmitt,*[a] Marcel Böhm,[a] Christian Ratzer,[a] Daniel Krügler,[a] Karl Kleinermanns,[a] Ivo Kalkman,[b] Giel Berden,[b] and W. Leo Meerts[b]

The rotationally resolved UV spectra of the electronic origins of five isotopomers of the phenol dimer have been measured. The complex spectra are analyzed using a fitting strategy based on a genetic algorithm. The intermolecular geometry parameters have been determined from the inertial parameters for both electronic states and compared to the results of ab initio calculations. In the electronic ground state, a larger hydrogen-bond length than in the ab initio calculations is found together with a smaller tilt angle of the aromatic rings, which shows a more pronounced dispersion interaction. In the electronically excited state, the hydrogen-bond length decreases, as has been found for other hydrogen-bonded clusters of phenol, and the two aromatic rings are tilted less toward each other.

1. Introduction

The phenol dimer is an ideal model system to study the very sensitive equilibrium between hydrogen bonding and dispersion interaction. The spectroscopy of complexes of phenol with different solvent molecules has been the subject of a plethora of publications in the last few decades. In most of these complexes phenol acts as a proton donor with respect to the solvent molecule, due to its acidic character. Phenol in its electronically excited state is a much stronger acid than in the ground state [pK_s(S$_1$)$=$6; pK_s(S$_0$)$=$9.8].[1] The phenol dimer takes a special position, since one of the cluster constituents acts as proton donor and the other as proton acceptor. Dispersive interactions between the aromatic rings are most likely to play an important role in the structure, while for most of the other phenol–X clusters (X$=$H$_2$O,[2–15] CH$_3$OH,[16–18] N$_2$,[19–24] NH$_3$,[25–34] CO[19,35]) the hydrogen bond is the main structure-determining parameter. Exceptions here are, of course, clusters of phenol with noble gases[36,37] or with CH$_4$,[38] which are stabilized by pure van der Waals interactions.

The first multiphoton ionization spectrum of the phenol dimer in a molecular beam was presented by Fuke and Kaya.[39] Later, the same authors showed that the electronic origin of the donor moiety is red-shifted by 303 cm^{-1} relative to the origin of bare phenol, while the acceptor origin is blue-shifted by 353 cm^{-1}.[40] Only the donor moiety of the dimer fluoresces, while the acceptor moiety could only be detected via ionization[41] or hole-burning schemes.[42] The electronic ground state has been investigated using dispersed fluorescence spectroscopy after excitation of the donor moiety. The intermolecular stretching vibration in the electronic ground state (109 cm^{-1}) and in the excited state of the donor (120 cm^{-1}) and the acceptor (106 cm^{-1}) have been found to be very similar. Hartland et al. performed ionization-loss stimulated Raman

spectroscopy, and discussed the observed vibrational frequency shifts for both donor and acceptor phenol in terms of the strength of the hydrogen bond.[43] The fluorescence lifetime of the donor moiety was determined to be 16 ns by Sur and Johnson using pump–probe photoionization.[3] Felker[44] and Connell et al.[45] determined the rotational constants of the phenol dimer using rotational coherence spectroscopy (RCS). As a consequence of the low temporal resolution of their experiment, the rotational constants reported by them are averaged over ground and electronically excited constants and no information on the geometry change upon electronic excitation was obtained. Later, Weichert et al.[46] performed an RCS experiment on the dimer with higher resolution and were able to extract the rotational constants of ground and excited states separately. Hobza et al.[47] performed ab initio calculations at the RI-MP2/TZVPP level of theory and found good

[a] Dr. M. Schmitt, M. Böhm, Dr. C. Ratzer, Dr. D. Krügler,$^+$
Prof. Dr. K. Kleinermanns
Institut für Physikalische Chemie
Universitätsstraße 26.43.02, 40225 Düsseldorf (Germany)
Fax: (+49) 211-81-5195
E-mail: mschmitt@uni-duesseldorf.de

[b] I. Kalkman, Dr. G. Berden,$^{++}$ Dr. W. L. Meerts
Molecular and Biophysics Group, Institute for Molecules and Materials
Radboud University Nijmegen
P.O. Box 9010, 6500 GL Nijmegen (The Netherlands)

[$^+$] Current address:
Bruker Daltonik GmbH, 28359 Bremen (Germany)

[$^{++}$] Current address:
FOM Institute for Plasma Physics Rijnhuizen
Edisonbaan 14, 3439 MN Nieuwegein (The Netherlands)

Supporting information for this article is available on the WWW under http://www.chemphyschem.org or from the author.

agreement with the experimental inertial parameters from ref. [46]. IR–UV double-resonance spectroscopy and stimulated Raman–UV double-resonance spectra of the phenol dimer were published by Ebata et al.[48] For the dimer, they found that the IR intensity of the OH stretching vibration of the donor moiety is four times larger than that of the acceptor moiety. Ebata et al. investigated the intramolecular vibrational relaxation (IVR) from OH stretching vibrations of the phenol dimer using picosecond IR–UV pump–probe spectroscopy.[49] They found a strong site dependence of the IVR rate. IVR of the donor site was found to occur much faster (5 ps) than that of the acceptor site (14 ps).

Prior to the determination of the cluster structure, the geometries of the constituents have to be known precisely. Phenol in the electronic ground state has been thoroughly investigated by microwave spectroscopy and a complete Kraitchman structure has been deduced by Larsen.[50] Christoffersen et al. calculated a shortening of the CO bond of 4.4 pm and an increase in the $C_6C_1C_2$ angle of 3.7° upon electronic excitation, by using the rotational constants obtained from a band contour analysis.[51] Ratzer et al. determined the structure of phenol in the S_1 state by a fit to the rotational constants of 12 isotopomers, which were obtained from rotationally resolved UV spectroscopy.[15]

Herein, the intermolecular geometry of the phenol dimer will be elucidated in both the S_0 and S_1 states on the basis of the rotational constants of five isotopomers. We measured the rotationally resolved electronic spectrum of the phenol dimer as early as 1995, but were not able at that time to extract the molecular constants from the spectra with the classical fitting procedure, which needs assignments of single rovibronic lines. In the meantime, we made progress in the automated fitting of complex spectra using a genetic algorithm (GA) approach. An additional motivation, to show the possibilities of this method in combination with rotationally resolved electronic spectroscopy, is stipulated in the following statement from a recent publication on the phenol dimer:[47] "The RCS technique is complementary to frequency-resolved spectroscopic techniques since it can be successfully applied to large systems, where the latter techniques are not applicable due to overlapping resonances. The phenol dimer is such an example, since until now the frequency spectra could not be assigned." In the following discussion we show how the development of the GA-based fitting strategy challenges this statement.

Experimental Section

The experimental setup for the rotationally resolved laser-induced fluorescence system is described in detail elsewhere.[17] Briefly, it consists of a ring dye laser (Coherent 899-21) operated with rhodamine 110, and pumped with 6 W of the 514-nm line of an Ar^+-ion laser. The light is coupled into an external folded ring cavity (Spectra Physics) for second harmonic generation. The molecular beam is formed by expanding phenol (or the respective isotopomers) by heating to 160 °C and seeding in 700 mbar of argon through a 100-μm hole into the vacuum. The atomic numbering for phenol used herein is given in Figure 1. [H₆]Phenol (99.5%) was purchased from Riedel de Haen and used without further purification. [7-
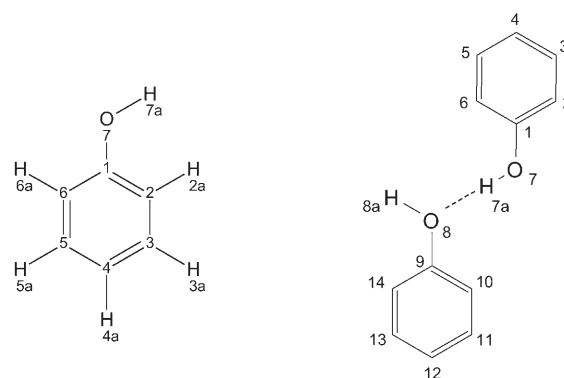
Figure 1. Atomic numbering of phenol and the phenol dimer. Both are drawn planar for reasons of clarity only and do not relate to the true structure.

D]phenol (d₁) was prepared by refluxing dried [H₆]phenol with an excess of D_2O (Merck, isotopic purity > 98.8%) three times followed by the removal of water. The isotopic purity of the sample was higher than 95%. The samples of [D₆]phenol (isotopic purity 99%) and [1-¹³C]phenol (isotopic purity > 99%) were purchased from Chemotrade and used without further purification.

The molecular beam machine consisted of three differentially pumped vacuum chambers that were linearly connected by two skimmers (1 and 3 mm, respectively) to reduce the Doppler width. The molecular beam was crossed at right angles in the third chamber with the laser beam 360 mm downstream of the nozzle. The resulting fluorescence was collected perpendicular to the plane defined by the laser and molecular beams by an imaging optics setup consisting of a concave mirror and two plano-convex lenses. The resulting Doppler width in this setup is 25 MHz (FWHM). The integrated molecular fluorescence is detected by a photomultiplier tube, the output of which is discriminated and digitized by a photon counter and transmitted to a PC for data recording and processing. The relative frequency is determined with a quasi-confocal Fabry–Perot interferometer. The absolute frequency was determined by recording the iodine absorption spectrum and comparing the transitions with the tabulated lines.[52]

2. The Genetic Algorithms

We used an automated fitting procedure for the rovibronic spectra, based on a genetic algorithm fit, which is described in detail in refs. [37] and [53]. The GA library PGAPack version 1.0 was used, which can run on parallel processors.[54] For the simulation of the rovibronic spectra, a rigid asymmetric rotor Hamiltonian is employed [Eq. (1)]:[55]
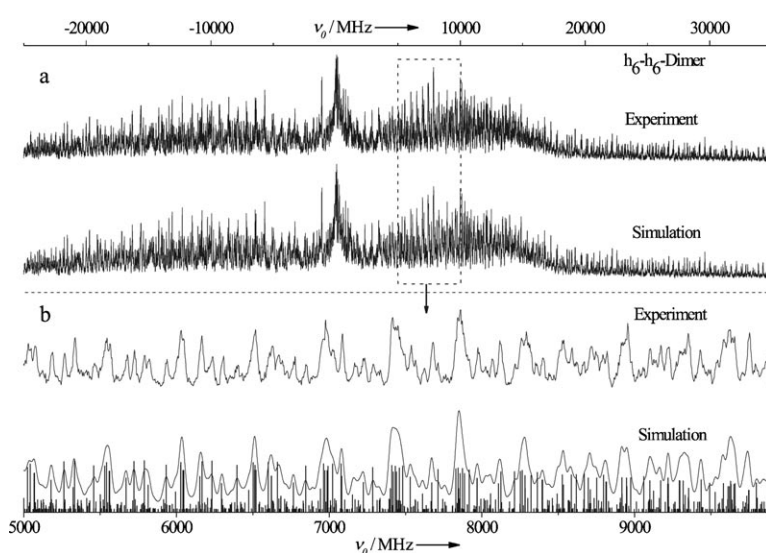
$$H = AP_a{}^2 + BP_b{}^2 + CP_c{}^2 \qquad (1)$$

where P_g ($g = a,b,c$) represents the components of the body-fixed angular momentum operator, and A, B, and C are the three rotational constants. The temperature dependence of the intensity is described by a two-temperature model [Eq. (2)]:[56]

$$n(E, T_1, T_2, w) = e^{-E/kT_1} + we^{-E/kT_2} \qquad (2)$$

where E is the energy of the lower state, k is the Boltzmann constant, w is a weighting factor, and T_1 and T_2 are the temperatures. The calculations were performed on maximum 64 processors (Intel Itanium 2, 1.3 GHz) of an SGI Altix 3700 system and on 64 processors (Intel Xeon, 3.4 GHz) of a Linux cluster. A typical fit with 64 processors takes less than 10 min. The genetic algorithm copies concepts from evolutionary processes such as sexual reproduction, selection, and mutation. For a detailed description of the GA as fitting algorithms, the reader is referred to the original literature on evolutionary or genetic algorithms.[57–59] The cost function used to describe the quality of the fit is defined in ref. [53].

3. Results and Discussion

Figure 2 shows the rovibronic spectrum of the electronic origin of the phenol dimer together with the best GA fit using the molecular parameters from Table 1. The lowest trace shows a zoomed part of the convoluted simulation along with the stick spectrum. What appear to be single lines in the spectrum are essentially clusters of up to 15 lines, which contribute with similar intensities. In this example the usefulness or even the indispensability of the GA-based fitting strategy in the automated assignment of such a congested spectrum is obvious. Given the large density of rovibronic lines, a classical assignment procedure seems to be hopeless or at least tedious.

The spectrum is fitted using a rigid rotor Hamiltonian with a two-temperature model. It is of mixed *abc* type and consists of about 13 000 lines in a range of 50 GHz. At a rotational temperature of about 5 K, more than 100 J states are populated with an intensity of at least 0.5 % of the strongest transition in the spectrum. The rotational constants for both electronic states, the origin frequencies, the polar angles defining the orientation of the transition dipole moment in the inertial frame, and the Lorentzian contribution to a Voigt profile with 25 MHz Gaussian are given in Table 1.

Figure 3 shows the rovibronic spectrum of the doubly deuterated dimer (d_1-d_1). The deuteration positions are 7a and 8a (see Figure 1). Due to incomplete deuteration, an additional weak band shows up, which can be assigned to a singly deuterated isotopomer in either the 7a (donor) or 8a (acceptor) position. In principle, there should also be the differently mono-deuterated counterpart, but despite intense scanning we could not spot an additional band. The observed singly deuterated isotopomer can be assigned to the donor deuterated species on the basis of the structural fits described in Section 3.1. The finding that only the donor deuterated isotopomer is observed

Figure 2. Experimental and fitted rovibronic spectra of the electronic origin of the h_6-h_6 isotopomer of the phenol dimer at 36 044.70 cm^{-1}. a) Full spectrum b) 5 GHz zoomed in, together with the stick spectrum. (The rotational constants from Table 1 are used).

Table 1. Molecular parameters of the electronic origin band of the phenol dimer as obtained from the genetic algorithm fit. The molecular constants from an RCS study[46] are given for comparison; their uncertainties are recalculated as 1σ values to be comparable with our results. Rotational constants, their differences, vibronic origins, and Lorentzian full linewidth contributions are given in MHz, angles are given in degrees.

	h_6-h_6	h_6-h_6[46]	d_1-d_1	d_1-h_6[a]	d_6-d_6	^{13}C-^{13}C
A''	1416.99(39)	1414.4(3)	1376.23(10)	1399.78(124)	1239.33(12)	1413.22(15)
B''	313.51(1)	313.7(4)	312.84(3)	312.72(6)	287.25(1)	311.84(2)
C''	288.11(1)	287.5(4)	286.44(2)	287.16(6)	264.63(1)	286.70(2)
ν_0	36 044.70(1)	36 044	36 047.56(1)	36 047.98(1)	36 217.50(1)	36 045.46(1)
ϕ	58.2(30)	66.9[b]	55.2(100)	66.6(23)	58.3(20)	57.4(30)
θ	29.5(30)	37.4[a]	35.7(100)	37.6(16)	40.0(35)	35.9(60)
$\Delta_{Lorentz}$	10(3)	–	10(3)	10(3)	10(3)	10(3)
Δ_A	10.71(1)	11.3(12)	4.55(1)	7.81(10)	4.28(2)	10.60(1)
Δ_B	−5.31(1)	1.6(40)	−3.95(1)	−5.63(1)	−3.93(1)	−5.25(1)
Δ_C	−5.82(1)	−12.2(35)	−4.76(1)	−5.99(1)	−4.90(1)	−5.76(1)

[a] Donor moiety deuterated. [b] Calculated from the alignment of the TDM, given in ref. [46].
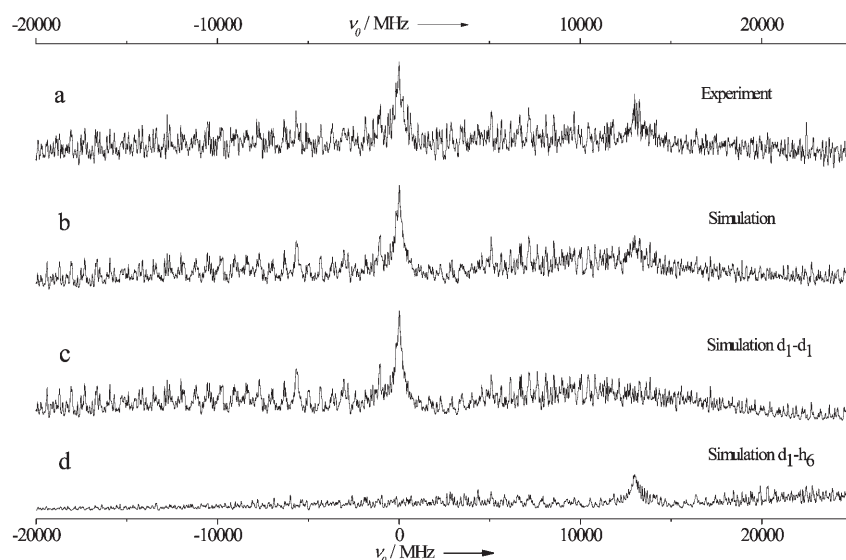
Figure 3. Rovibronic spectra of the electronic origins of the d_1-d_1 and d_1-h_6 isotopomers of the phenol dimer at 36 047.56 and 36 047.98 cm^{-1}. a) Experimental spectrum b) full simulated spectrum using the rotational constants from Table 1 c) simulated spectrum of the d_1-d_1 isotopomer; d) simulated spectrum of the d_1-h_6 isotopomer.

experimentally is in agreement with microwave investigations of the ethylene oxide–water cluster by Caminati et al.[60] They showed that deuteration in the hydrogen bond (the donor position in the case of the phenol dimer) results in a lower zero-point vibrational energy, which favors this isotopomer. The second trace of Figure 3 shows the overall result of the GA fit; the lower two traces show the individual fits of the two isotopomers. The molecular parameters of the fit are summarized in Table 1.

Since the deuterations in the mono- and bideuterated isotopomer take place close to the b and c inertial axes, their effect on the B and C rotational constants is small. Another isotopomer which has a much more pronounced effect on all rotational constants is the fully deuterated d_6-d_6 isotopomer. The rovibronic spectrum of the electronic origin at 36 217.50 cm^{-1} is shown in Figure 4, along with the best fit. The lowest trace also includes the stick spectrum which, even more than in the case of the h_6-h_6 isotopomer, shows the indispensability of the GA for assignment of such a complex spectrum. The resulting molecular parameters are compiled in Table 1. Since it is impossible to find single rovibronic lines in the experimental spectrum, which are needed for an assigned line fit to assess the

standard deviation of the parameters, we employed a different scheme for the estimation of the standard deviation. The variances and covariances of the fitted parameters are determined from the results of several independent runs of the GA using different initial seeds.

The spectrum of the phenol dimer in which the C1 and C9 carbon atoms (see Figure 1) are replaced by ^{13}C is shown in the Supporting Information. Since the amount of substance was very small (200 mg [1-^{13}C]phenol) and evaporated fast through the nozzle, the spectral range covered is smaller than that for the other isotopomers. The results are given in Table 1.

The rotational constants in Table 1 have larger standard deviations than expected for a molecule with a well-defined Hamiltonian and a spectrum with good signal-to-noise ratio. Part of this standard deviation results from the large number of overlapping lines, which makes it difficult even for the GA to find a unique solution. Another important contribution is the non-consideration of centrifugal distortion effects in the fit. We could not improve the fit by introducing the five centrifugal distortion constants from Watson's A-reduced Hamiltonian. An upper limit of 30 kHz on the largest constant is approximated, which leads only to small corrections of the rotational constants.
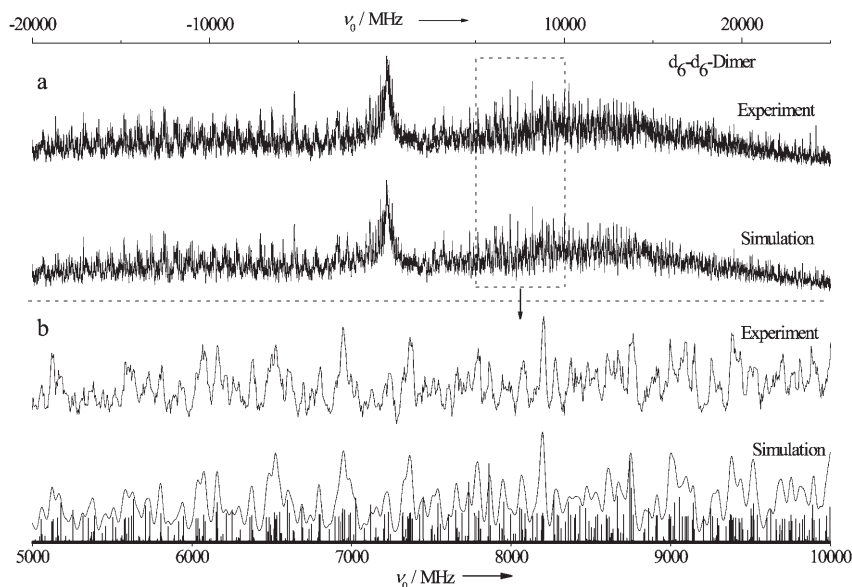
Figure 4. Experimental and fitted rovibronic spectra of the electronic origin of the d_6-d_6 isotopomer of the phenol dimer cluster at 36 217.50 cm^{-1}. a) Full spectrum b) 5 GHz zoomed in, together with the stick spectrum. (The rotational constants from Table 1 are used).

A comparison of the molecular parameters for the h_6-h_6 isotopomer to the values from the RCS study by Weichert et al.[46] shows good agreement for the rotational constants of the electronic ground state, but quite large deviations for the electronically excited state. Nevertheless, given the large uncertainties for the excited-state rotational constants in ref. [46], which were attributed to the fact that no excited-state C'-type transients have been allocated in the RCS spectrum, the excited-state constants also agree within these limits. The only systematic difference seems to be in the ground-state A rotational constants of the RCS experiment and the present study, which are significantly different outside the quoted uncertainties.

The excited-state lifetime of the h_6-h_6 isotopomer is determined to be 16 ± 4 ns from a Lorentzian contribution of 10 ± 3 MHz to the total linewidth. Although this value agrees with the value of Sur and Johnson of 16 ns,[3] which was obtained by pump–probe photoionization, it has a much higher uncertainty, which is unusual for the GA-based line fit, as this fit includes all lines even if they are overlapping. A closer look at the stick spectra in Figures 2 and 4 reveals the probable reason for this problem. Since many rovibronic transitions contribute to one line in the experimental spectrum, the slightest deviations of the rotational constants from the true values lead to an apparent broadening or narrowing of the observed lines. In cases where too many transitions overlap to form the observed lines, the determination of the lifetime from a deconvolution of the Voigt profile results in less reliable values for the Lorentzian contribution, thus not allowing for an exact determination of the lifetime.

3.1. Determination of the Structure

A first approach to the change of the cluster structure upon electronic excitation can be made using the center of mass (COM) distance of the monomer moieties in the cluster, as has been shown by Connell et al.[45] and later by Weichert et al.[46] The COM distance of the two monomer moieties is given by Equation (3):

$$R = \sqrt{\frac{\sum_g I_g^{\text{Dimer}} - \sum_g I_g^{\text{Donor}} - \sum_g I_g^{\text{Acceptor}}}{2\mu}} \qquad (3)$$

where μ is the reduced mass of donor and acceptor, and the I_g

are the respective moments of inertia, described by their superscripts, which are calculated from experimentally determined rotational constants. The COM distance for the h_6-h_6 and the d_1-d_1 clusters in the ground state are calculated using the same monomer rotational constants for the acceptor and donor moieties. They are obtained from the fit of microwave transitions given in ref. [61] to the Hamiltonian used in the study by Ratzer et al.[15] in order to be based on the same model as the dimer rotational constants. The ground-state COM distance of the d_6-d_6 cluster is calculated using the rotational constants from ref. [15] based on the microwave spectra of Forest and Dailey.[62] For the mixed d_1-h_6 cluster the microwave spectra from ref. [61], and for the ^{13}C-^{13}C dimer from ref. [50], are used to evaluate the inertial data. The standard deviations for the COM distances were calculated using the full covariance matrices obtained from the fits of the monomer moieties to the microwave transitions and from the fit of the dimer, described above. They represent pure statistical errors. Systematic deviations, for example, from the assumption of unaltered monomer geometries upon complexation, are not taken into account and might be larger than the quoted standard deviations.

Assuming local excitation in the donor moiety, the COM distance in the electronically excited state can also be calculated. Therefore, we use the rotational constants of the electronically excited state from the high-resolution UV spectroscopy of phenol[15] for one of the monomer moieties and the ground-state rotational constants for the other one. The S_1-state rotational constants of the ^{13}C isotopomer have so far not been published.[63] Table 2 summarizes the results for the observed isotopomers. The differences between the COM distances of the different isotopomers can be attributed to the shift of the COM in each monomer moiety due to isotopic substitution. In all cases an increase of the COM distance of the monomer moieties upon electronic excitation is found.

The program *pKrFit*[15] was used to determine the intermolecular structure of the phenol dimer in the S_0 and S_1 states from the rotational constants given in Table 1. *pKrFit* uses a gradient-based χ^2 minimizer as well as a GA-based global optimizer.[64] While the speed of the gradient method is appealing, the main disadvantage is the possibility of being trapped in a local minimum. The GA library[54] was applied in minimization mode, and thus directly used the correspondingly defined χ^2 value as cost function.

Table 2. COM distance [pm] of the five observed isotopomers of the phenol dimer in the ground and electronic excited states. Standard deviations of the distance differences are typically smaller than those of the individual ones due to high correlations between S_0 and S_1 state values. The lower three rows give the COM distances calculated from the fitted pseudo-r_s structures in Table 3.

	h_6-h_6	d_1-d_1	d_1-h_6[a]	d_6-d_6	^{13}C-^{13}C
S_0	525.126(1)	521.730(19)	523.645(54)	527.0091(77)	523.848(22)
S_1	530.187(5)	525.591(15)	529.000(42)	531.4022(36)	528.871(22)
Δ	5.061(3)	3.861(2)	5.455(10)	4.3931(7)	5.022(4)
S_0[b]	524.99	521.80	523.44	526.91	524.02
S_1[c]	531.85	528.61	530.88	534.31	530.77
S_1[d]	531.64	527.72	529.90	533.27	530.57

[a] Donor moiety deuterated. [b] $S_0(r_s)$ structure. [c] $S_1(r_s)$ structure of model 1. [d] $S_1(r_s)$ structure of model 2.

We performed two different fits of the structural parameters to the rotational constants.[65] The first fit neglects the vibrational contributions from the different isotopomers completely and is based on the assumption [Eq. (4)]:

$$I_g^0 = I_g^e(r_0) \tag{4}$$

where I_g^0 are the experimentally determined zero-point averaged moments of inertia with respect to the inertial axes g. The functions $I_g^e(r_0)$ are calculated from the structural parameters r_0 using rigid-molecule formulas.

The second method uses a "Kraitchmans Ansatz" for individual coordinates to obtain the r_s structure of the molecule.[66,67] The approximation assumes equal vibrational contributions for all isotopomers [Eq. (5)]:

$$I_g^0 = I_g^e(r_s) + \frac{1}{2}\varepsilon_{0g} \tag{5}$$

where the three ε_{0g} contain the average vibrational contributions with respect to the inertial axes g. The original Kraitchman method is only applicable to singly or symmetrically substituted isotopomers. In our case the structure is fitted to the moments of inertia, given by Equation (5). The resulting structure is called a pseudo-r_s structure. As the three ε_{0g} have to be fitted, three inertial parameters are lost for the structure determination.

Additional information from the spectra, which is used in the fit of the intermolecular dimer structure, is contained in the transition dipole moment (TDM) orientations of the different conformers. Since the orientation of the TDM does not change upon isotopic substitution, it is only subject to changes upon rotation of the inertial system. These rotations depend on the structure of the cluster and can be used to improve the fit of the geometry. Although the differences of the orientation angles are small, the structure fit is more stable and the correlations between the parameters are reduced if the TDM directions of the isotopomers are included in the fit, as has been shown in a recent publication.[64]

The relative orientation of the two phenol moieties can be described by six intermolecular coordinates: one distance of two selected atoms (one from each monomer), two angles, and three dihedral angles, which describe the relative orientation of the monomer moieties. Thus, the 15 rotational constants from five isotopomers are sufficient for the determination of the intermolecular geometry under the assumption of known monomer geometries.

For the determination of the intermolecular cluster structure in the ground state, the experimentally determined S_0 monomer structure of Larsen[50] was used for both donor and acceptor phenol. Table 3 reports the structural parameters from the fit. The assumption of unchanged monomer geometries has to be made due to a lack of sufficient data that can be used to fit the monomer geometries. Nevertheless, in many cases the approximation of unaltered monomer geometries in the cluster has been proven to be reasonably good. The results of the fit of an r_0 and pseudo-r_s structure to the rotational constants is given in Table 3. Both structures are very similar, which arises from the fact that the vibrational corrections ε_{0g} are small. Two different views of the resulting pseudo-r_s structure are also shown in the upper part of Figure 5. An additional measure for the quality of the applied model is the compari-
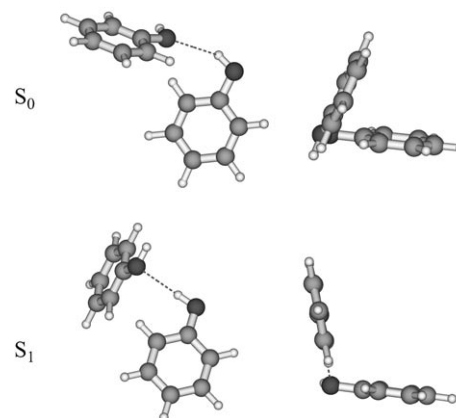
Figure 5. Top: two different views of the S_0 (r_s) geometry of the phenol dimer from Table 3. Bottom: same viewing angles for the excited-state structure. The depicted geometry is the pseudo-r_s structure of model 1 in Table 3.

Table 3. Comparison of experimentally determined r_0 and r_s geometry parameters of the phenol dimer in the S_0 and S_1 states. All distances are given in pm, angles and dihedral angles in degrees, and pseudo-r_s parameters $\varepsilon_{0a,b,c}$ in $\mu\text{Å}^2$. For the fit of the intermolecular structure of the dimer in the S_1 state, we used the monomer geometries from a CIS/6-311G(d,p) calculation of the dimer in model 1 and a locally excited donor moiety in model 2.

			Model 1		Model 2	
	$S_0(r_0)$	$S_0(r_s)$	$S_1(r_0)$	$S_1(r_s)$	$S_1(r_0)$	$S_1(r_s)$
$r(H_{7a}O_8)$	235.4(49)	236.9(54)	229.3(86)	229.0(87)	174.7(16)	174.4(16)
$a(O_7H_{7a}O_8)$	150.6(18)	150.5(20)	179.9(10)	179.9(1)	179.9(1)	179.9(1)
$a(C_9O_8H_{7a})$	138.6(15)	139.8(14)	104.0(19)	104.1(20)	135.5(8)	135.7(9)
$d(O_8H_{7a}O_7C_1)$	19.6(45)	9.4(47)	46.8(21)	46.9(21)	63.9(9)	63.4(9)
$d(C_9O_8H_{7a}O_7)$	63.5(46)	62.8(46)	−131.4(21)	−131.2(20)	−115.1(9)	−114.8(9)
$d(C_{10}C_9O_8H_{7a})$	−181.0(19)	−178.2(22)	−104.0(19)	−104.1(29)	−101.6(14)	−101.5(14)
ε_{0a}	–	0.0(10)[a]	–	0.0[b]	–	0.0[b]
ε_{0b}	–	3.11(13)	–	3.11[b]	–	3.11[b]
ε_{0c}	–	1.9(2)	–	1.9[b]	–	1.9[b]

[a] Estimated uncertainty, since fit converged to lower parameter boundary. [b] Fixed to the ground-state value.

son of the COM distances, which are obtained directly from the moments of inertia of the monomer moieties and the cluster [Eq. (3)] and the COM distance calculated for the fitted structures. The respective values are given in Table 2. For the electronic ground state the difference is about 0.1 pm, which shows the reliability of the assumptions made in the course of the fit.

The determination of the S_1-state structure is much more difficult, since the geometry changes in the monomer moieties are not known. We first performed a local fit with the intermolecular geometry of the ground state as starting parameters. The geometry of the monomer moieties in the S_1 state is derived from a CIS/6-311G(d,p) optimized geometry of the cluster. In this fit (model 1 in Table 3), the structural parameters of the monomer moieties obtained from the ab initio calculations of the cluster are retained, while the six intermolecular geometry parameters are fitted. The COM distances of the different isotopomers of the monomer moieties have been calculated from the fitted S_1 structure, as for the ground state. The deviation from the directly calculated COM distances is larger (typically 2–3 pm, compared to 0.1 pm for the ground state).

We also tried to fit the structure of the dimer in the excited state using the excited-state structure of the phenol monomer determined by Ratzer et al.[15] for the donor moiety, and the unaltered S_0 structure of Larsen[50] for the acceptor moiety. Two approximations are made at this level: the monomer moieties in the cluster are unaltered and the excitation takes place locally in the donor moiety. The first approximation has already been discussed for the ground-state geometry. The second one seems to be more arguable. A purely local excitation in one of the aromatic rings is quite unlikely, since a considerable dispersive interaction has to be considered for the ground state, which will dramatically change upon electronic excitation of one of the phenol moieties. A local fit of the intermolecular parameters using the model of localized excitation in the donor moiety (model 2 in Table 3) leads to a strongly shortened O⋯O hydrogen bond in comparison to the fit using model 1 (see Table 3).

In the next step we tried the global fit of the intermolecular parameters, as for the ground state. For the excited state we found geometry minima, which depend strongly on the chosen geometry of the monomer moieties, thus leading to no stable fits. Furthermore, all geometries obtained with the global fitter show large changes compared to the ground state. In nearly all cases even the hydrogen bond is broken in favor of a "T-shaped" structure.

4. Conclusions

The intermolecular structure of the phenol dimer in the electronic ground state can be described as hydrogen bonded, with one phenol moiety acting as proton donor and the other as proton acceptor. The rings are more tilted than expected from a pure translinear arrangement, as found, for example, for the phenol–water cluster. This deviation is a consequence of the additional dispersive interactions between the two aromatic rings, as has already been pointed out by Hobza et al.[47]

Nevertheless, there are important differences between the structure we determined on the basis of five different isotopomers and the results of the MP2/6-31G(d) counterpoise-corrected calculations from ref. [47]. To properly compare the two structures, we determined the intermolecular distances and angles, which were defined in ref. [47], in our experimentally determined geometry. The results are presented in Table 4.

Table 4. Comparison of experimentally determined r_s geometry parameters of the phenol dimer in the S_0 state with the values of the MP2/6-31G(d) calculation from ref. [47]. All distances are given in pm, angles and dihedral angles in degrees.

	r_s	MP2/6-31G(d,p)[47]
$r(O_7{\cdots}O_8)$	321	295
$a(C_1O_7O_8)$	112.7	90.0
$a(O_7O_8C_9)$	117.1	134.2
$a(O_7O_8H_{8a})$	116.0	132.1
$d(C_2C_1O_7O_8)$	5.7	−2.4
$d(C_1O_7O_8C_9)$	63.0	−56.1
$d(O_7O_8C_9C_{10})$	12.2	−19.8

First of all, the $O_7{\cdots}O_8$ distance obtained from our structure is larger than that from the ab initio calculations. Given the fact that the *A* rotational constant of the ab initio calculations is too large by about 40 MHz, and the O⋯O hydrogen bond is oriented more or less along the inertial *a* axis, this difference is easily understandable. All other angles and dihedral angles are quite similar, but point to a slightly more bent structure than that predicted by the ab initio calculations. The apparently large difference in the dihedral angle $d(C_1O_7O_8C_9)$ only describes two different orientations of the acceptor ring relative to the donor ring. In one of the structures, the acceptor is below, and in the other it is above, the donor plane. These orientations are equivalent with respect to the intermolecular interactions and describe the same molecule. Thus, to conclude the results for the electronic ground state, we find a weaker hydrogen-bonding interaction than predicted by the ab initio calculations, but a stronger dispersive interaction between the aromatic rings. The applicability of the model employed in this study (same geometry for both acceptor and donor) can be checked using the COM distances calculated from Equation (3). If this assumption is correct, the COM distances calculated from Equation (3) and from the best structure fit using *pKrFit* should coincide within their uncertainties. For all isotopomers, we found close coincidence between the COM distances calculated in these two manners.

Since the assumption of local excitation in just one monomer moiety seems to be incorrect, the results for the determination of the structure of the electronically excited state are more doubtful. We tried several different models to describe the excitation in the dimer, but all of these models did not converge to a physically meaningful structure. The most logical assumption for the excited-state structures of the monomer moieties seems to be a local excitation in the donor moiety, with the geometry of the donor equal to the excited-state

structure of the phenol monomer and that of the acceptor moiety equal to the ground-state structure. All models based on this assumption led to dimer structures in which the hydrogen bond is broken and that could be better described as "T-shaped". Nevertheless, from low-resolution laser-induced fluorescence and hole-burning experiments on the dimer, it is known that the intermolecular stretching vibration has similar frequencies in the S_0 and S_1 states.[42] A break of the hydrogen bond upon electronic excitation therefore seems to be unrealistic.

Based on the monomer geometries of a CIS/6-311G(d,p) calculation, we fitted the intermolecular geometry parameters to the rotational constants of the excited state (model 1, Table 3). While the intermolecular geometry of the cluster is by no means expected to be correct using a method that completely neglects the dispersion interaction of the aromatic rings, the monomer geometries in such a cluster are generally well-described. A shorter hydrogen-bond length (229.3 pm) than in the electronic ground state (235.4 pm) is found. The tilt of the aromatic rings toward each other is smaller, that is, the dispersive interaction seems to be smaller in the excited state. This opening of the dimer upon electronic excitation is further supported by the comparison of COM distances of the monomer moieties in the S_0 and S_1 states. While the hydrogen-bond distance decreases upon excitation, the COM distance increases for all isotopomers. This is only possible if the tilt angle of both rings increases (see Figure 5). A fit assuming local excitation in one of the phenol moieties (model 2, Table 3) leads to a very short hydrogen bond (174.7 pm), which seems not to be realistic. The same procedure as for the electronic ground state has been used to check for reliability of the applied models. For the excited state, the COM distances calculated from the moments of inertia and from the fitted structures differ more than those for the excited state, thus showing that the fit still contains model errors. Both model 1 and model 2 show nearly the same deviations, which makes it impossible to favor one of them.

The results for the excited-state structure depend strongly on the chosen model, and need further refinement using information from isotopomers other than the ones used in this study, to estimate the changes in the monomer moieties upon electronic excitation. Nevertheless, decreases in hydrogen-bond length and in the tilt angle of the aromatic ring are found as common characteristics of all S_1-state structures. Until now no reliable theoretical method has been available for correctly describing the sensitive equilibrium between hydrogen bonding and dispersion interaction in the electronically excited state.

Acknowledgements

[1] G. Granucci, J. Hynes, P. Millié, T.-H. Tran-Thi, *J. Am. Chem. Soc.* **2000**, *122*, 12243–12253.

[2] H. Abe, N. Mikami, M. Ito, *J. Phys. Chem.* **1982**, *86*, 1768–1771.

[3] A. Sur, P. M. Johnson, *J. Chem. Phys.* **1986**, *84*, 1206–1209.

[4] R. J. Stanley, A. W. Castleman, Jr., *J. Chem. Phys.* **1991**, *94*, 7744–7756.

[5] R. J. Lipert, S. D. Colson, *J. Chem. Phys.* **1988**, *89*, 4579–4585.

[6] M. Schütz, T. Bürgi, S. Leutwyler, T. Fischer, *J. Chem. Phys.* **1993**, *98*, 3763–3776.

[7] G. Berden, W. L. Meerts, M. Schmitt, K. Kleinermanns, *J. Chem. Phys.* **1996**, *104*, 972–982.

[8] M. Gerhards, M. Schmitt, K. Kleinermanns, W. Stahl, *J. Chem. Phys.* **1996**, *104*, 967–971.

[9] M. Schmitt, C. Jacoby, K. Kleinermanns, *J. Chem. Phys.* **1998**, *108*, 4486–4495.

[10] R. M. Helm, H. P. Vogel, H. J. Neusser, *J. Chem. Phys.* **1998**, *108*, 4496–4504.

[11] T. Ebata, M. Furukawa, T. Suzuki, M. Ito, *J. Opt. Soc. Am. B* **1990**, *7*, 1890–1897.

[12] O. Dopfer, G. Reiser, K. Müller-Dethlefs, E. W. Schlag, S. D. Colson, *J. Chem. Phys.* **1994**, *101*, 974–989.

[13] T. Watanabe, T. Ebata, S. Tanabe, N. Mikami, *J. Chem. Phys.* **1996**, *105*, 408–419.

[14] S. Tanabe, T. Ebata, M. Fujii, N. Mikami, *Chem. Phys. Lett.* **1993**, *215*, 347–352.

[15] C. Ratzer, J. Küpper, D. Spangenberg, M. Schmitt, *Chem. Phys.* **2002**, *283*, 153–169.

[16] A. Courty, M. Mons, B. Dimicoli, F. Piuzzi, V. Brenner, P. Millié, *J. Phys. Chem. A* **1998**, *102*, 4890–4898.

[17] M. Schmitt, J. Küpper, D. Spangenberg, A. Westphal, *Chem. Phys.* **2000**, *254*, 349–361.

[18] A. Westphal, C. Jacoby, C. Ratzer, A. Reichelt, M. Schmitt, *Phys. Chem. Chem. Phys.* **2003**, *5*, 4114–4122.

[19] D. M. Chapman, K. Müller-Dethlefs, J. B. Peel, *J. Chem. Phys.* **1999**, *111*, 1955–1963.

[20] S. R. Haines, W. D. Geppert, D. M. Chapman, M. J. Watkins, C. E. H. Dessent, M. C. R. Cockett, K. Müller-Dethlefs, *J. Chem. Phys.* **1998**, *109*, 9244–9251.

[21] M. S. Ford, S. R. Haines, I. Pugliesi, C. E. H. Dessent, K. Müller-Dethlefs, *J. Electron Spectrosc. Relat. Phenom.* **2000**, *112*, 231–239.

[22] A. Fujii, M. Miyazaki, T. Ebata, N. Mikami, *J. Chem. Phys.* **1999**, *110*, 11125–11128.

[23] N. Solca. O. Dopfer, *Chem. Phys. Lett.* **2000**, *325*, 354–359.

[24] M. Schmitt, C. Ratzer, W. L. Meerts, *J. Chem. Phys.* **2004**, *120*, 2752–2758.

[25] J. A. Syage, J. Steadman, *J. Chem. Phys.* **1991**, *95*, 2497–2510.

[26] M. F. Hineman, D. F. Kelley, E. R. Bernstein, *J. Chem. Phys.* **1993**, *99*, 4533–4538.

[27] G. A. Pino, G. Grégoire, C. Dedonder-Lardeux, C. Jouvet, S. Martrenchard, D. Solgadi, *Phys. Chem. Chem. Phys.* **2000**, *2*, 893–900.

[28] G. Grégoire, C. Dedonder-Lardeux, C. Jouvet, S. Martrenchard, A. Peremans, D. Solgadi, *J. Phys. Chem. A* **2000**, *104*, 9087–9090.

[29] G. Grégoire, C. Dedonder-Lardeux, C. Jouvet, S. Martrenchard, D. Solgadi, *J. Phys. Chem. A* **2001**, *105*, 5971–5976.

[30] M. Schmitt, C. Jacoby, M. Gerhards, C. Unterberg, W. Roth, K. Kleinermanns, *J. Chem. Phys.* **2000**, *113*, 2995–3001.

[31] H. T. Kim, R. J. Green, J. Qian, S. L. Anderson, *J. Chem. Phys.* **2000**, *112*, 5717–5721.

[32] S. Ishiuchi, M. Saeki, M. Sakai, M. Fujii, *Chem. Phys. Lett.* **2000**, *322*, 27–32.

[33] S. Ishiuchi, K. Daigoku, M. Saeki, M. Sakai, K. Hashimoto, M. Fujii, *J. Chem. Phys.* **2002**, *117*, 7077–7082.

[34] S. Ishiuchi, K. Daigoku, M. Saeki, M. Sakai, K. Hashimoto, M. Fujii, *J. Chem. Phys.* **2002**, *117*, 7083–7093.

[35] S. R. Haines, C. E. H. Dessent, K. Müller-Dethlefs, *J. Chem. Phys.* **1999**, *111*, 1947–1954.

[36] S. Ullrich, G. Tarczay, K. Müller-Dethlefs, *J. Phys. Chem. A* **2002**, *106*, 1496–1503.

[37] W. L. Meerts, M. Schmitt, G. Groenenboom, *Can. J. Chem.* **2004**, *82*, 804–819.

[38] B. B. Champagne, J. F. Pfanstiel, D. W. Pratt, R. C. Ulsh, *J. Chem. Phys.* **1995**, *102*, 6432–6443.

[39] K. Fuke, K. Kaya, *Chem. Phys. Lett.* **1982**, *91*, 311–314.

[40] K. Fuke, K. Kaya, *Chem. Phys. Lett.* **1983**, *94*, 97–101.

[41] O. Dopfer, G. Lembach, T. G. Wright, K. Müller-Dethlefs, *J. Chem. Phys.* **1993**, *98*, 1933–1943.

[42] M. Schmitt, U. Henrichs, H. Müller, K. Kleinermanns, *J. Chem. Phys.* **1995**, *103*, 9918–9928.

[43] G. V. Hartland, B. F. Henson, V. A. Venturo, P. M. Felker, *J. Phys. Chem.* **1992**, *96*, 1164–1173.

[44] P. M. Felker, *J. Phys. Chem.* **1992**, *96*, 7844–7857.

[45] L. L. Connell, S. M. Ohline, P. W. Joireman, T. C. Corcoran, P. M. Felker, *J. Chem. Phys.* **1992**, *96*, 2585–2593.

[46] A. Weichert, C. Riehn, B. Brutschy, *J. Phys. Chem. A* **2001**, *105*, 5679–5691.

[47] P. Hobza, C. Riehn, A. Weichert, B. Brutschy, *Chem. Phys.* **2002**, *283*, 331–339.

[48] T. Ebata, T. Watanabe, N. Mikami, *J. Phys. Chem.* **1995**, *99*, 5761–5764.

[49] T. Ebata, M. Kayano, S. Sato, N. Mikami, *J. Phys. Chem. A* **2001**, *105*, 8623–8628.

[50] N. W. Larsen, *J. Mol. Struct.* **1979**, *51*, 175–190.

[51] J. Christoffersen, J. M. Hollas, G. H. Kirby, *Proc. R. Soc. London Ser. A* **1968**, *307*, 97–110.

[52] S. Gerstenkorn, P. Luc, *Atlas du Spectre d'Absorption de la Molécule d'Iode 14800–20000 cm^{-1}*, CNRS, Paris, **1986**.

[53] J. A. Hageman, R. Wehrens, R. de Gelder, W. L. Meerts, L. M. C. Buydens, *J. Chem. Phys.* **2000**, *113*, 7955–7962.

[54] D. Levine, PGAPack V1.0; PgaPack can be obtained via anonymous ftp from: ftp://ftp.mcs.anl.gov/pub/pgapack/pgapack.tar.z, **1996**.

[55] H. C. Allen, P. C. Cross, *Molecular Vib-Rotors*, Wiley, New York, **1963**.

[56] Y. R. Wu, D. H. Levy, *J. Chem. Phys.* **1989**, *91*, 5278–5284.

[57] J. H. Holland, *Adaption in Natural and Artificial Systems*, University of Michigan Press, Ann Arbor, **1975**.

[58] D. E. Goldberg, *Genetic Algorithms in Search, Optimisation and Machine Learning*, Addison-Wesley, Reading, **1989**.

[59] I. Rechenberg, *Evolutionsstrategie: Optimierung technischer Systeme nach Prinzipien der biologischen Evolution*, Frommann-Holzboog, Stuttgart, **1973**.

[60] W. Caminati, P. Moreschini, I. Rossi, P. G. Favero, *J. Am. Chem. Soc.* **1998**, *120*, 11144–11148.

[61] T. Pedersen, N. W. Larsen, L. Nygaard, *J. Mol. Struct.* **1969**, *4*, 59–77.

[62] H. Forest, B. P. Dailey, *J. Chem. Phys.* **1966**, *45*, 1736–1746.

[63] D. Krügler, M. Schmitt, unpublished results.

[64] M. Schmitt, D. Krügler, M. Böhm, C. Ratzer, V. Bednarska, I. Kalkman, W. L. Meerts, *Phys. Chem. Chem. Phys.* **2006**, *8*, 228–235.

[65] J. K. G. Watson, A. Roytburg, W. Ulrich, *J. Mol. Spectrosc.* **1999**, *196*, 102–119.

[66] J. Kraitchman, *Am. J. Phys.* **1953**, *21*, 17–24.

[67] C. Costain, *J. Chem. Phys.* **1958**, *29*, 864.